Hydrocarbon-degrading microbial populations in permanently cold deep-sea sediments in the NW Atlantic.

Oyeboade Adebayo[1*], Srijak Bhatnagar[1,5], Jamie Webb[2], Calvin Campbell[3], Martin Fowler[2], Natasha M. MacAdam[4], Adam Macdonald[4], Carmen Li[1] and Casey R.J. Hubert[1*]

[1] Department of Biological Sciences, University of Calgary, AB T2N 1N4, Canada
[2] Applied Petroleum Technology (Canada), Calgary, AB T2N 1Z6, Canada
[3] Geological Survey of Canada-Atlantic, Dartmouth, NS B3B 1A6, Canada
[4] Nova Scotia Department of Natural Resources and Renewables, Halifax, NS B2H 4G8, Canada
[5] Faculty of Science and Technology, Athabasca University, Athabasca, AB T9S 3A3, Canada

*Corresponding authors: oye.adebayo@ucalgary.ca; chubert@ucalgary.ca

Running title: Deep seabed hydrocarbon biodegradation

Abstract

Permanently cold deep-sea sediments (2500-3500 m water depth) with or without indications of thermogenic hydrocarbon seepage were exposed to naphtha to examine the presence and potential of aerobic hydrocarbon-degrading microbial populations. Monitoring these microcosms for volatile hydrocarbons by GC-MS revealed sediments without *in situ* hydrocarbons responded more rapidly to naphtha amendment than hydrocarbon seep sediments overall, but seep sediments removed BTEX compounds more readily. Naphtha-driven aerobic respiration was more evident in surface sediment (0-20 cmbsf) than deeper anoxic layers (>130 cmbsf) that responded less rapidly. In all cases, enrichment of Gammaproteobacteria included lineages of *Oleispira*, *Pseudomonas*, and *Alteromonas* known to be associated with marine oil spills. On the other hand, taxa known to be prevalent *in situ* and diagnostic for thermogenic hydrocarbon seepage in deep sea sediment did not respond to naphtha amendment. This suggests a limited role for seep-associated populations in the context of oil spill biodegradation.

Keywords**:** deep sea sediments, hydrocarbon biodegradation, microbial community composition, Gammaproteobacteria

1. Introduction

Offshore oil exploration has been happening for over 100 years (Hyne, 2001) with recent advances in drilling technology seeing activities extending farther offshore into deeper waters (EIA, 2016). Ultra deep-water operations in the Gulf of Mexico include Perdido at 2,450 m and Stones at 2,900 m, with similarly deep discoveries off the coast of Brazil such as the Carcana site in 2,030 m (Offshore Technology, 2017). Deep water presents challenging operational environments as illustrated by the Deepwater Horizon (DWH) oil blowout that occurred while producing oil in approximately 1,500 m water (Hazen et al., 2010; Camilli et al., 2011; Shukla and Karki 2016). This highlights the importance of understanding the microbial ecology of the

deep sea, both with respect to baseline microbial communities (Joye, 2015; Ferguson et al., 2023) and the potential these microbiomes harbour for the biodegradation of spilled oil.

Hydrocarbonoclastic bacteria in marine ecosystems can derive carbon and energy from the degradation of petroleum hydrocarbons (Hazen et al., 2010, Kimes et al, 2014, Yang et al., 2016, Berry and Gutierrez, 2017). These bacteria have been observed to proliferate following oil spills and thus represent catalytic potential that can be harnessed for bioremediation (Yakimov et al., 2007, Acosta-Gonzalez et al., 2015, Joye et al., 2016, Duran and Cravo-Laureau, 2016; Yang et al., 2016). Reasons for the presence of oil-degrading microbial populations in the ocean include widespread occurrences of natural seabed hydrocarbon seepage (Head et al., 2006), yet it is unclear whether bacteria commonly understood to be hydrocarbonoclastic (Berry and Gutierrez, 2017; Gutierrez et al., 2013; Sanni et al., 2015) are a guild that overlaps with dominant microbial populations inhabiting hydrocarbon seep sediments in the deep sea (Dong et al., 2019, 2020; Chakraborty et al., 2020; Li et al., 2023).

Most published studies following the DWH interrogated the response of microbial communities in the water column to the introduction of spilled oil and gas (Hazen et al., 2010; Redmond and Valentine., 2012; Yang et al., 2016). Additional research showed 2-15% of the oil released from the Macondo wellhead eventually became deposited onto the deep-sea sediments via marine oil snow sedimentation and floc accumulation (Passow et al., 2012; Valentine et al. 2014; Chanton et al. 2015). Hydrocarbons deposited in marine sediments become absorbed into the sediment organics impacting ecosystem functioning (Karickhoff et al., 1979; Eadie et al., 1982, McGroddy and Farrington., 1995; Coates et al., 1997, Cravo-Laureau and Duran., 2014). Nearby sediments investigated following the DWH blowout revealed oil deposition penetrating the top 5 cm of the seabed (Joye et al., 2014). Natural hydrocarbon seeps on the other hand receive inputs of petroleum compounds from below via slower advection as part of geological petroleum systems (Joye, 2020). As a result, deep sea sediments experiencing hydrocarbon seepage are enriched in particular taxa, including *Caldatribacteriota*, *Aminicenantes* and *Campilobacterota* (Chakraborty et al. 2020; Li et al. 2023). Whether or not these taxa would be involved in the biodegradation of petroleum compounds entering the seabed from above in an oil spill scenario requires further investigation.

Temperature is another factor that controls the fate of oil in the marine environment. Physical and chemical properties of hydrocarbon compounds as well as the metabolic rates catalyzed by hydrocarbonoclastic microbes are influenced by temperature. The deep sea is generally very cold, with temperatures close to 0°C (Yasuhara and Danovaro 2016). To investigate the potential for psychrophilic aerobic hydrocarbon biodegradation in a deep-sea setting, sediments with and without in situ hydrocarbons were incubated with naphtha (low molecular weight hydrocarbons including short- and long-chain alkanes and monoaromatic hydrocarbons) at 4°C for 100 days and compared with each other to test the hypothesis that cold seep sediments are primed for biodegradation.

2. Materials and methods

2.1. Seismic description

Seismic interpretation was performed on the Shelburne (NS24-S006-003E) and Tangier (NS24-B071-001E) 3D surveys using Schlumberger's Petrel software platform to assess potential piston

coring locations based on amplitude anomalies and the presence of direct hydrocarbon indicators (DHIs). Geophysical Reports for the 3D seismic surveys can be accessed here: https://cnsopbdigitaldata.ca/dmc-summary/. DHIs were inferred to be associated with possible seabed seeps on the basis of potential hydrocarbon migration pathways in the form of faults from deeper in the subsurface up to the seafloor (Figure 1B, C).

2.2. Study site and sampling

Sampling was conducted onboard the CCGS *Hudson* in June and July in 2016. Sediments from four stations 16-06, 16-13, 16-18 and 16-21 were sampled via piston coring along the Scotian slope off the coast of Nova Scotia in the NW Atlantic Ocean (Fig 1). Within a few hours of core retrieval, sediments from these cores were sub-sampled and used to establish experimental microcosms that were amended with hydrocarbons and incubated at 4°C. Surface sediments (0-20 cmbsf) were sampled from 16-06, 16-13 and 16-18, and deeper sediments were also subsampled at 134-141 cmbsf (16-18) and 142-148 cmbsf (16-21).

2.3. Sulfate measurements

Sulfate concentrations in sediment porewater were measured at several depths following porewater extraction by centrifugation of a small aliquot of wet sediment (ca. 500 mg) taken from cores that were longitudinally sectioned on board the ship. Porewater was obtained by centrifugation. Initial sulfate measurements were made onboard by monitoring barium sulfate using the "USEPA SulfaVer 4" method with the Pocket Colorimeter II (Hach, Canada) and barium chloride ampules (AccuVac Ampules, Hach Canada). This rapid estimation of sulfate profiles and hence overall redox zonation in the sediments guided the choice of deeper sediment layers from cores 0018 and 0021. Additional sediment aliquots sampled in parallel were immediately stored on board in a -20°C freezer. These samples were eventually thawed and centrifuged similarly, allowing for sulfate measurements using a Dionex ICS 5000 reagent-free ion chromatography system (Thermo Scientific, CA, USA) equipped with an anion-exchange column (Dionex IonPac AS22; 4 × 250 mm; Thermo Scientific, USA), an EGC-500 eluent generator cartridge, and a conductivity detector. The eluent was Na_2CO_3 (4.5 mM) and $NaHCO_3$ (1.4 mM) with a flow rate of 1.2 mL min^{-1} at 30 °C column temperature.

2.4. Hydrocarbon gas and liquid analysis in piston core sediment samples

Sediment was collected immediately after core retrieval from near the base of each core for hydrocarbon gas analysis by placing 200-300 g of sediment into a 500 ml Isojar that was flushed with nitrogen before sealing. Headspace gas aliquots were transferred to exetainers as 0.1-1.0 ml, arranged in a Gerstel MPS2 autosampler and injected into an Agilent 7890 RGA GC equipped with Molsieve and Poraplot Q columns, a flame ionisation detector (FID) and a thermal conductivity detector (TCD). Hydrocarbons were measured by FID. To measure liquid hydrocarbons, separate samples were wrapped in aluminium foil and stored at -20°C on board. Following extraction of organic matter, liquid hydrocarbons from this fraction were measured using a HP7890 A GC instrument equipped with a CP-Sil-5 CB-MS column (length 30 m, i.d. 0.25 mm, film thickness 0.25 µm) using synthesized $C_{20}D_{42}$ compound as an internal standard.

2.5. Sediment microcosms amended with low-molecular weight hydrocarbons.

Microcosms set up under oxic conditions (i.e., with air in the headspace) were established to assess how aerobic microbial communities in different surface sediments respond to exogenous hydrocarbon exposure. Sediment from 0-20 cmbsf was sampled from cores 16-06, 16-13 and 16-18. Deeper sediment layers corresponding to the sulfate reduction zone were sampled from cores 16-18 (134-141 cmbsf) and 16-21 (142-148 cmbsf), to additionally test for the presence of more deeply buried aerobic microbial communities and their ability to respond to hydrocarbon exposure in oxic microcosms. Microcosms consisted of 6 ml of sediment and 25 mL of ONR7a medium (Dyksterhouse et al., 1995) added to sterile 50 mL serum bottles with air in the headspace that were sealed with septa and aluminum crimp tops. Bottles were amended with 0.2% (v/v) naphtha, which is a qualitative reference blend of low molecular weight alkanes and aromatics. Heat killed controls (autoclaved microcosms), unamended controls (artificial seawater and sediment without naphtha amendment) and uninoculated controls (no sediment) were also established and incubated in parallel. All microcosms were kept static and incubated as triplicate bottles in the dark at 4°C for between 100 and 106 days.

2.6. Microbial respiration in microcosms

Headspace carbon dioxide and oxygen levels were measured at different sampling points using an Agilent 7890B gas chromatograph equipped with a thermal conductivity detector (TCD) and according to a protocol described elsewhere (Novotnik et al. 2019). The instrument operated under the following parameters: TCD temperature: 200°C, reference flow: He 40 mL/min. FID: Heater T: 200°C, Air flow 400 ml/min, H_2 fuel flow 50 ml/min. Column 1: 0.5 m × 1/8″ Hayesep N (80/100 mesh); Column 2: 6′ × 1/8″ Hayesep N (80/100 mesh); Column 3: 8′ × 1/8″ MS5A (60/80 mesh). A reference gas mix from Praxair (Mississauga, Canada) was used for calibration.

2.7. Hydrocarbon consumption in microcosms

Volatile hydrocarbons were analyzed by injecting 100 µl headspace sample from each microcosm directly into an Agilent 6890N gas chromatograph/mass spectrometer (GC/MS) with a model 5973 inert mass selective detector and HP-5MS capillary column (30 m length, 0.25 mm internal diameter and 0.25 µm film thickness). The injector temperature was 250°C, and He carrier gas had a flow rate of 1 ml min^{-1} and split/splitless ratio of 1:10. The GC temperature program was 40°C for 5 min, then ramping up at 5°C min^{-1} to 85°C (Abu Laban et al., 2015). The GC/MS was run in full scan monitoring mode for m/z = 50-500. Headspace hydrocarbon depletion was assessed using the GC-MS method described by Prince and Suflita (2007) using 1,1,3-trimethylcyclohexane as the conserved internal standard (Townsend et al., 2004). The percentage of specific hydrocarbon (HC) compounds remaining in the headspace was calculated as $(A_{sample}/C_{sample})/(A_{heat\ killed}/C_{heat\ killed}) \times 100$, where A and C represent specific HC compounds and an internal standard respectively (Tan et al., 2015).

2.8. DNA extraction and 16S rRNA gene sequencing

Total genomic DNA was extracted from microcosm sediment slurries using the DNeasy PowerSoil kit (Qiagen, Valencia, CA, USA) according to manufacturer protocols. Extracted DNA was quantified using a Qubit 2.0 Fluorometer (Invitrogen). The V3–V4 hypervariable region of Bacterial and Archaeal 16S rRNA genes was amplified by polymerase chain reaction (PCR) using the universal primers Pro341F and Pro805R (Takahashi et al., 2014). Amplicon libraries were generated as triplicate twenty-five microliter reactions of 5-10 ng/μL DNA template, 1 μM of each primer, and 12.5 μL 2x KAPA HiFi Hot Start (Kapa Biosystems, Boston, USA). Amplification was performed using a Nexus GSX1 Master cycler (Eppendorf, Germany) as follows: initial denaturation at 94°C for 2 min, followed by 35 cycles of denaturation at 94°C for 30 sec, annealing at 58°C for 60 sec, and extension at 72°C for 60 sec, and final elongation at 72°C for 5 min. Triplicate PCR products were pooled and prepared for Illumina paired end sequencing using Illumina's dual indexing protocol. Sequencing was performed using an in-house benchtop Illumina MiSeq sequencer (Illumina, San Diego, CA, USA).

2.9. DNA sequence analysis

Primer and adapter removal of raw demultiplexed reads was performed using cutadapt v1.16 (Martin, 2011). Primer trimmed sequences were quality checked and merged in DADA2 v1.9.0 (Callahan et al., 2016). Using the filterAndTrim function in DADA2, forward and reverse reads were trimmed to 280 bp and 220 bp, with filtering for reads with no ambiguous bases (maxN=0). Any reads with a quality score below 8 were truncated (trunqQ = 8). All suspect phiX sequences from the Illumina run were removed (rm.phix=TRUE) and only reads with expected error less than 2 for forward and 4 for reverse reads, were retained (max EE = c(2,4)). Two million high quality random forward and reverse reads that passed these filters were used to learn the error rates. Using error profiles of forward and reverse reads, libraries were merged using the mergePairs function in DADA2. From these merged reads amplicon sequence variants (ASVs) were inferred using makeSequenceTable function, followed by chimera removal using removeBimeraDenovo function. Chimera-free SVs were then assigned taxonomy using assignTaxonomy function with Silva nr training set v128 and a minimum bootstrap of 80. The deepest assigned taxonomy of each sequence variant was chosen to depict the taxonomic classification.

The ASV table generated was then consolidated at the genus level and used in Divnet (Willis and Martin, 2022) within the R software package to calculate alpha diversity indices with the parameters, seed=2021 and base=ASV 46. Differential abundance analysis was performed on a table with all ASVs using *differentialTest* function of Corncob (Martin et al 2020). With a seed set to 2021 reads, all differential abundance analyses were carried out using Wald test with bootstrapping and a false detection rate of 0.05, for each experimental parameter and combinations (e.g., hydrocarbon amendment, comparison between cores, etc). Using this approach, a set of statistically significant differentially abundant ASVs was determined. The abundance of these ASVs was plotted using package ggplot2 v 2.2.1 (Wickham 2016).

Sequences for six ASVs suspected to belong to genera considered to be obligate hydrocarbonoclastic bacteria (Yakimov et al., 2007) were used in BLAST searches of the NCBI nr database. Hits with ≥99% sequence identity to these six 16S rRNA gene sequences were compiled and aligned using SINA aligner, (Pruesse et al., 2012) with *Sulfolobus islandicus*

(AY247900.1) as an outgroup. Phylogenetic tree reconstruction used RaxML (Stamatakis 2014) with Gamma livelihood and GTR models, and iTOL for visualization.

2.10. Data availability

Raw sequencing data used in this study can be accessed through NCBI BioProject Acc# PRJNA1014963

3. Results

3.1: Geophysical and geochemical evidence of hydrocarbon seepage

Geophysical imagery revealed sites 16-18 and 16-21 have subsurface acoustic features considered to be direct hydrocarbon indicators (DHIs), faulting, and a seafloor irregularity (Figure 1; Table 1). Site 16-13 exhibits faults to surface but no apparent DHI (Fig 1C). In agreement with these geophysical observations, the strongest geochemical evidence for sedimentary hydrocarbon gases and liquids was observed in cores 16-18 and 16-21 (Fig 2A, B). Furthermore, downcore sulfate concentration profiles differed distinctly between sampling sites (Fig 2C). A much steeper drop in sulfate concentration was observed in cores 16-18 and 16-21, where sulfate was completely depleted by 250 cmbsf; this is consistent with hydrocarbons providing additional substrates elevated sulfate reduction in these sediments. In contrast, cores 16-06 and 16-13 exhibited no marked drop in sulfate, with relatively flat profiles throughout the top 500 cm of the seabed.

3.2. Aerobic respiration coupled to hydrocarbon removal at 4°C in sediment microcosms.

Carbon dioxide production and oxygen depletion in the headspace of microcosms were monitored periodically as a proxy for naphtha biodegradation. Figure 3 shows that during the surface sediment incubations, O_2 depletion and CO_2 production did not differ significantly between naphtha-amended and unamended control microcosms until after 100 days for 16-13 and 16-18 sediments. On the other hand, sediment 16-06 showed a more rapid response to the naptha amendment (see ANOVA significance values in Table S1). In agreement with O_2 and CO_2 observations, GC-MS analysis revealed decreasing concentrations of certain volatile hydrocarbon compounds in the headspace of naphtha-amended microcosms compared to no-sediment controls with identical naphtha amendment (Fig 3G, H & I). However, naphtha-amended microcosms were not substantially different in headspace hydrocarbon profiles compared to heat killed controls (ANOVA values in Table S2).

Deeper anoxic sediment layers exhibited similar potential for aerobic hydrocarbon biodegradation. Naphtha-amended microcosms established with the sediment from the sulfate reduction zone (130 -150 cmbsf) of cores 16-18 and 16-21 gave rise to CO_2 production that was more extensive than 16-18 surface sediments (0–20 cmbsf), but still not as extensive as the surface sediments from cores 16-06 and 16-13 where hydrocarbons were not detected in situ. Deeper sediment microcosms did not show substantial differences in the depletion of headspace oxygen concentration when compared to controls (Fig. S1).

Hydrocarbon analysis of naphtha-amended microcosms revealed different degrees of hydrocarbon compound depletion relative to heat killed controls between 50 and 100 days of incubation at 4°C. In order to inoculate the microcosms with fresh sediment, incubations were established within hours of sampling on board the ship where headspace measurements of initial volatile hydrocarbon concentrations were not possible; hence the percentage of removal between the period of 50 and 100 days is used for comparison. In general, a greater variety of hydrocarbon compounds were depleted in surface sediment incubations compared to incubation with sediments from deeper anoxic layers (Fig 4; Fig. S2). Toluene, ethylbenzene and xylene were primarily removed from microcosms established with sediment from cores 16-18 and 16-21 where hydrocarbons were detected in situ, whereas microcosms with sediment from core 16-06 showed a depletion of the larger aromatic compounds cyclohexane, ethyl cyclohexane and methyl cyclopentane.

3.3. DNA sequence analysis

Amplicon sequencing resulted in 98 paired end libraries from different microcosms and incubation time points for the various treatments and controls. This resulted in 4,985,354 raw reads (2 × 300 bp), with individual library sizes varying from 1,104 to 542,925 reads (median 63,330 reads). After quality processing and merging of read pairs, the total dataset comprised 2,022,825 reads, with libraries ranging from 3,415 to 245,687 reads (median 24,682 reads) (Table S3). Chimera-free amplicon sequence variants (ASVs) detected by DADA2 differed in length. To avoid spurious ASVs while retaining diversity, all the ASVs shorter than 380 bp or longer than 435 bp were removed. The remaining 14,754 ASVs received taxonomic assignments resulting in 1,195 archaeal, 13,364 bacterial and 91 eukaryotic ASVs as well as 104 ASVs that were unclassified. Corncob identified 29 non-redundant statistically significant ASVs with differential abundance patterns across all experimental parameters that are elaborated on in the next section.

3.4. Shifts in microbial community composition during sediment incubations.

Comparing microcosms established with sediment from core 16-18 (*in situ* hydrocarbons detected) with the 16-06 and 16-13 microcosms (no hydrocarbons detected in the cores), revealed very few differences (Fig 5). Increases in the relative abundance of *Oleispira* ASV_9, *Pseudomonas* ASV_1 and *Alteromonas* ASV_3 was evident in all surface sediment incubations, compared to being detectable but at low levels (<10%) in parallel incubations without naphtha (Fig. S3). A notable difference was *Colwellia* ASV_6 being significantly elevated in relative abundance only microcosms from cores 16-06 and 16-13, whereas ASV_51 *Moritella* was only detected in microcosms established with 16-06 and 16-18 sediment, albeit at lower relative abundance. Interestingly, the relative abundance of *Oleispira* ASV_9 increased over time in naphtha-amended microcosm from cores 16-06, 16-13, 16-18 but not in parallel unamended microcosms, whereas *Oleispira* ASV_7 exhibited a divergent pattern by increasing in unamended microcosms from core 16-13 sediment (Figure S3) but not in corresponding naphtha-amended microcosms (Fig 5).

Comparison of microbial communities in oxic naphtha-amended microcosms inoculated with sediment from deeper anoxic layers of cores 16-18 and 16-21 (Fig. S4) revealed general differences relative to the surface sediment incubations. Increased relative abundance of *Pseudomonas* ASV_11 was pronounced in the deeper sediment microcosms (both 16-18 and 16-21). This effect was most dramatic in 16-18 sediment (the only site with parallel incubations of surface and deeper sediment from the same core) where ASV_11 was not enriched in surface sediments but reached >30% in the deeper sediment incubation. In contrast the increase in *Olesipira* ASV_9 in 16-18 surface sediment microcosms was not observed in deeper sediment from the same core (ASV 9 not detected), however this organism did get enriched in the incubation of deeper sediment from core 16-21. The other two populations enriched in all surface sediments, *Pseudomonas* ASV_1 and *Alteromonas* ASV_3, both increased over time in the deeper sediment incubations, where they were similarly among the most prevalent ASVs (Fig. S4).

4. Discussion

Oxygen availability is key amidst abiotic and biotic factors that influence hydrocarbon degradation in marine sediments. Microbes preferentially deplete available oxygen during respiration (Breitburg et al., 2010) and as oxygen availability is diminished, alternative electron acceptors, such as sulfate, are used (Lam and Kuypers, 2011). Seabed study sites used here presented not only habitats differing in sulfate concentrations but also proximity to potential hydrocarbon seeps. Additional input of carbon in the form of the hydrocarbon fluids flowing up from below facilitates a more rapid depletion of oxygen leading to the use of sulfate as an alternate electron acceptor at shallower intervals given its high concentration in seawater and marine sediment porewater. The presence of hydrocarbon liquids and gases in cores 16-18 and 16-21 are consistent with the steeper sulfate profiles in these locations. Accordingly, these sites enabled a comparison of biodegradation in deep sea sediments with and without exposure to natural sources of hydrocarbons.

Despite levels of in situ hydrocarbons in cores 16-18 and 16-21 being higher than in cores 16-06 and 16-13 (Figure 2), these hydrocarbon seep sediments did not exhibit a more rapid biodegradation response in 4°C microcosm experiments. Naphtha amendment in surface sediments resulted in enhanced respiration in samples from the top of cores 16-06 and 16-13 relative to surface sediment from core 16-18 where hydrocarbons were detected (Figure 3). Compared to controls incubated in parallel without hydrocarbon amendment, significantly higher carbon dioxide production ($P = 0.03$) and oxygen depletion ($P = 0.001$) were recorded in 0006 sediment amended with naphtha after 60 days. This rapid <60-day response was not observed in naphtha-amended surface sediments from site 16-13, but by 100 days activity in the 16-13 microcosms was comparable to the 0006 microcosms, i.e., >10 mM CO_2 production, whereas only 3 mM CO_2 production was measured in the naphtha-amended incubation of surface sediment from core 0018 (Fig 3; Fig S1; Table S1). These experiments do not provide evidence to suggest that prior exposure to hydrocarbons due to seepage leads to an enhanced biodegradation response.

Enrichment of Gammaproteobacterial groups in all microcosms reflects observations in other marine systems in response to oil spills. Gammaproteobacteria were not among the taxa deemed to be diagnostic for thermogenic hydrocarbon seepage in the deep-sea sediments at this

study site (Li et al. 2023) or at Gulf of Mexico seabed hydrocarbon seeps (Chakraborty et al. 2020) where lineages including *Caldatribacteria*, *Aminicenantes* and *Campilobacterota* are common indicators. Instead, naphtha resulted in the enrichment of *Oleispira*, *Alteromonas* and *Pseudomonas* as being among the most important populations in the biodegradation response. Some of these gammaproteobacterial groups, such as *Oleispira*, are considered obligate hydrocarbonoclastic taxa (Yakimov et al., 2007) that are otherwise minor bacterial constituents of the pristine (oil-free) marine systems (Radwan et al., 2019). Different *Oleispira* strains were enriched in both naphtha amended (ASV_9) and unamended (ASV_7) 4°C incubations over the course of 100 days (Fig. 5 and S3), calling into question the designation of this genus as being 'obligately' hydrocarbonoclastic. Non-detection of *Oleispira* ASV_9 at the onset of the incubations (week 0) in all but one of the sediments (i.e., the deeper anoxic layer of core 16-21; Fig. S3) is consistent with hydrocarbon-degrading taxa being minor constituents with low in situ abundance. On the other hand, *Alteromonas* ASV_3, which was enriched in the presence of naphtha in all five microcosms spanning surface and deeper sediments, could be detected in three out of the five unincubated in situ sediment samples (i.e., week 0) at 0.04 to 0.17% relative sequence abundance. This is consistent with its 16S rRNA gene phylogeny indicating a close relationship with the known hydrocarbon degrader *Alteromonas naphthalenivorans* (Fig. S5). Instances of *Alteromonas* detection in situ include both 16-18 and 16-21 sediments where hydrocarbons were detected in the sediment cores (Fig. 1). Detection and enrichment of *Alteromonas*, *Pseudomonas* and other aerobic hydrocarbon degrading Gammaproteobacteria both in surface sediment and down to 148 cmbsf in these two locations (Figure 1A, B) suggests that these aerobic hydrocarbon degraders persist in a viable state during sediment burial to this depth, which lasted thousands of years in this area given the low sedimentation rate of 0.4 mm y^{-1} (Normandeau & Campbell, 2020).

Metagenomic and metatranscriptomic analyses conducted during the unmitigated release of oil for 84 days during DWH blowout revealed alkane degradation was a dominant hydrocarbon-degrading pathway coinciding with Gammaproteobacteria including *Pseudomonas* being dominant members of the community (Mason et al., 2012). In our study, an increased relative abundance of different *Pseudomonas* ASVs was observed in oxic naphtha-amended microcosms, corresponding to headspace depletion of alkanes and aromatic compounds, as has been reported for other members of this genus (Whyte et al., 1997). Toluene removal was especially prevalent in the 16-18 and 16-21 microcosms during 50-100 days, corresponding with increased abundance of *Pseudomonas* ASVs (Fig.4; Fig. S2). More rapid hydrocarbon metabolism may be explained by the observed natural hydrocarbon seepage at this location (Figure 1B). This could be relevant in the context of deep marine ecosystems like this study site and the DWH location in the Gulf of Mexico where there will be reduced weathering of light hydrocarbons in released crude oil due to the cold seawater with resultant higher concentrations of volatile toxic compounds such as BTEX (Brakstad et al., 2017). Widespread capacity for alkane biodegradation in the marine microbiome may not depend solely on the presence of natural hydrocarbon seeps. Alkane production by marine phototrophs exerts more widespread selective pressure for alkane biodegradation (Lea-Smith et al. 2015; Love et al. 2021). For aromatic hydrocarbons, seabed seeps may be a more likely point of introduction into the marine environment, resulting in 'priming' the marine microbiome for aromatic metabolism. Despite the overall slower response to naphtha amendment in the seep sediments, as described above, aromatic hydrocarbons were more readily consumed by the microbial communities enriched from the 16-18 and 16-21 sediments (Fig. 4; Fig. S3) where there is prior exposure to

thermogenic hydrocarbons (Figs. 1, 2). *Pseudomonas* spp. are well documented for their ability to degrade BTEX (Chicca et al., 2020) with the *Pseudomonas* ASVs in this study being closely related to those in other hydrocarbon-degrading systems (Fig. S5). For example, enrichment of *Alteromonas* in similar cold deep sea enrichment cultures amended with crude oil has also been linked to the degradation of aromatic compounds (Cui et al. 2008).

Permanently cold deep-sea sediments and their incubation with hydrocarbons at 4°C also expand knowledge of marine biodegradation processes and populations that operate at low temperatures. While *Oleispira*, *Alteromonas*, *Pseudomonas* and other 'usual suspects' within the Gammaproteobacteria are typically considered mesophiles, it is inferred from their enrichment here and their close phylogenetic relationships to bacteria from cold environments (Fig. S5) that these strains are psychrophilic inhabitants of the deep sea. Many psychrotolerant and some psychrophilic strains of *Pseudomonas* have been isolated (Canion et al., 2013; Kim et al., 2013; Kosina et al., 2013). Other studies have similarly shown that *Pseudomonas* spp. are found in low abundance across a range of cold environments and become dominant under stress, such as acute hydrocarbon exposure (Farrell et al., 2003; Aislabe et al., 2006; Yergeau et al., 2012). Enrichment of *Oleispira* ASVs in naphtha-amended microcosms is similarly unsurprising. Gregson et al. (2020) highlight that *Oleispira* shares many traits with other described genera of well-known marine obligate hydrocarbon degraders like *Alcanivorax* (Yakimov *et al*., 1998) and *Thalassolituus* (Yakimov *et al*., 2004) including marine origin, respiratory metabolism and ability to metabolise aliphatic alkanes and their derivatives. However, in contrast to other so-called obligate genera, *Oleispira antarctica* was shown to exhibit a broad growth temperature optimum between 1°C and 15°C (Yakimov *et al*., 2003) suggesting a potential for *Oleispira* spp. to dominate microbial communities due to their ecological competitiveness in cold environments (Hazen *et al*., 2010; Mason *et al*., 2012; Kube et al., 2013).

5. Conclusions

Microcosm experiments with deep sea sediments sampled from sites with and without background thermogenic hydrocarbon seepage did not support the hypothesis that prior exposure to hydrocarbons would lead to enhanced biodegradation. The capacity for the biodegradation of spilled petroleum compounds by marine microbial communities is often explained by the presence of natural hydrocarbon seeps in the seabed. Chemosynthetic ecosystems fuelled by thermogenic hydrocarbons highlight an important role for microbial populations capable of oxidizing these compounds as primary producers in the seabed (Dong et al 2019; 2020). Despite this premise, bacterial groups like *Oleispira*, *Alteromonas*, *Pseudomonas* and other members of the Gammaproteobacteria that typically respond to oil spills or oil-amendment enrichment experiments, like the ones performed here, differ from the signature microbial groups that define cold seep sediments such as *Caldatribacteria*, *Aminicenantes* and *Campilobacterota*. In the present study, none of the latter groups became enriched when sediments were exposed to low molecular weight hydrocarbons (naphtha) over a 100-day period. Instead, relatively rare psychrophilic Gammaproteobacteria responded to acute hydrocarbon exposures, supporting and expanding the widespread importance of these aerobic hydrocarbon-degrading bacteria across a range of marine oil pollution scenarios.

Credit author statement

Oyeboade Adebayo – Conceptualization; Formal analysis; Investigation; Methodology; Writing-Original Draft; Writing-Review & Editing; Visualization

Srijak Bhatnagar – Data curation; Formal analysis, Writing-Review & Editing, Visualization

Jamie Webb – Formal analysis

Calvin Campbell – Project administration; Resources; Supervision

Martin Fowler – Formal analysis; Writing-Review & Editing

Natasha M. MacAdam – Formal analysis

Adam MacDonald – Project administration; Resources; Supervision

Carmen Li – Investigation

Casey R.J. Hubert – Conceptualization; Funding acquisition; Supervision; Writing-Review & Editing

Acknowledgements

This research was supported by funds from the Campus Alberta Innovates Program (CAIP) chair program, Genome Canada, and the Marine Environment Observation Prediction and Response (MEOPAR) network. Partnerships with Genome Atlantic, Genome Alberta, the Government of Nova Scotia and Natural Resources Canada are gratefully acknowledged. Sampling aboard CCGS *Hudson* was made possible by its captain and crew, and collaborative support of Natural Resources Canada. Project management and support were provided by Dr Rhonda Clark and Carey Ryan.

Declaration of competing interest

Authors declare that they have no known competing financial interests or personal relationships that could influence the work reported in this paper.

Appendix: Supplementary data

References

Abu Laban, N., Dao A, and Foght, J. (2015). DNA stable isotope probing of oil sands tailings pond enrichment cultures reveals different key players for toluene degradation under methanogenic and sulfidogenic conditions. *FEMS Microbiol Ecol*, DOI: 10.1093/femsec/fiv039.

Acosta-González, A., Martirani-von Abercron, S. M., Rosselló-Móra, R., Wittich, R. M., and Marqués, S. (2015). The effect of oil spills on the bacterial diversity and catabolic function in coastal sediments: a case study on the Prestige oil spill. *Environ. Sci. Pollut. Res*. 22, 15200-15214.

Aislabie, J., Saul, D.J., and Foght, J.M. (2006). Bioremediation of hydrocarbon-contaminated polar soils. *Extremophiles* 10: 171–179.

Berry, D., and Gutierrez T. (2017) Evaluating the Detection of Hydrocarbon-Degrading Bacteria in 16S rRNA Gene Sequencing Surveys. *Front. Microbiol*. 8:896. doi:10.3389/fmicb.2017.00896

Brakstad, O.G., Lofthus, S., Ribicic, D., and Netzer, R. (2017). Biodegradation of petroleum oil in cold marine environments. In Psychrophiles: From Biodiversity to Biotechnology. R. Margesin (ed.), Springer International Publishing. DOI 10.1007/978-3-319-57057-0_27

Breitburg, D.L., Crump, B.C., Dabiri, J.O., and Gallegos, C.L. (2010) Ecosystem engineers in the pelagic realm: alteration of habitat by species ranging from microbes to jellyfish. *Integr Comp Biol* 50: 188–200.

Callahan, B., McMurdie, P., Rosen, M. *et al.* DADA2: High-resolution sample inference from Illumina amplicon data. *Nat Methods* **13**, 581–583 (2016). https://doi.org/10.1038/nmeth.3869

Camilli R, Di Iorio D, Bowen A, Reddy CM, Techet AH, Yoerger DR, Whitcomb LL, Seewald JS, Sylva SP, Fenwick J. (2011). Acoustic measurement of the Deepwater Horizon Macondo well flow rate. Proceedings of the National Academy of Sciences 109: 20235–20239.

Canion, A., Prakash, O., Green, S.J., Jahnke, L., Kuypers, M.M., and Kostka, J.E. (2013) Isolation and physiological characterization of psychrophilic denitrifying bacteria from permanently cold Arctic fjord sediments (Svalbard, Norway). *Environ Microbiol* 15: 1606–1618

Chakraborty A, Ruff SE, Dong X, Ellefson ED, Li C, Brooks JM, McBee J, Bernard BB, Hubert CRJ (2020). Hydrocarbon seepage in the deep seabed links subsurface and seafloor biospheres. PNAS 117, 11029-11037. doi.org/10.1073/pnas.2002289117

Chanton, J., Zhao, T., Rosenheim, B.E., Joye, S., Bosman, S., Brunner, C., Yeager, K.M., Diercks, A.R., Hollander, D., (2015). Using natural abundance radiocarbon to trace the flux of petrocarbon to the seafloor following the Deepwater Horizon oil spill. *Environ. Sci. Technol*. 49, 847–854.

Chicca, Ilaria, et al. “Degradation of BTEX Mixture by a New Pseudomonas Putida Strain: Role of the Quorum Sensing in Modulation of the Upper BTEX Oxidative Pathway.” *Environmental Science and Pollution Research International*, vol. 27, no. 29, 2020, pp. 36203–14, https://doi.org/10.1007/s11356-020-09650-y.

Coates, J. D., Woodward, J., Allen, J., Philp, P., and Lovley, D. R. (1997). Anaerobic degradation of polycyclic aromatic hydrocarbons and alkanes in petroleum-contaminated marine harbor sediments. *Appl. Environ. Microbiol*. 63: 3589-3593.

Cravo-Laureau, C. and Duran, R. (2014). Marine coastal sediements microbial hydrocarbon degradation processes: contribution of experimental ecology in the omicsera. *Front. Microbiol*. 5, 39.

Cui, Zhisong, et al. "Biodiversity of Polycyclic Aromatic Hydrocarbon-Degrading Bacteria from Deep Sea Sediments of the Middle Atlantic Ridge." *Environmental Microbiology*, accepted 19 March, 2008., vol. 10, no. 8, 2008, pp. 2138–49, https://doi.org/10.1111/j.1462-2920.2008.01637.x.

Dong, X., Greening, C., Rattray, J.E. Chakraborty A, Chuvochina M, Mayumi, D, Dolfing J, Li C, Brooks JM, Bernard BB, Groves RA, Lewis IA, Hubert CRJ (2019). Metabolic potential of uncultured bacteria and archaea associated with petroleum seepage in deep-sea sediments. *Nat Commun* 10, 1816 (2019). https://doi.org/10.1038/s41467-019-09747-0

Dong X, Rattray JE, Campbell DC, Webb J, Chakraborty A, Adebayo, O, Matthews S, Li C, Fowler M, Morrison NM, MacDonald A, Groves RA, Lewis IA, Wang SH, Mayumi, D, Greening, C, Hubert CRJ (2020) Thermogenic hydrocarbon biodegradation by diverse depth-stratified microbial populations at a Scotian Basin cold seep. Nature Communications 11, 5825. doi.org/10.1038/s41467-020-19648-2

Duran, R., and Cravo-Laureau, C (2016) Role of environmental factors and microorganisms in determining the fate of polycyclic aromatic hydrocarbons in the marine environment *FEMS Microbiol. Rev.* 40, 814–830, doi: 10.1093/femsre/fuw031

Dyksterhouse SE, Gray JP, Herwig RP, Cano Lara J, Staley JT. (1995). *Cycloclasticus pugetii gen. nov., sp.nov., an aromatic hydrocarbon-degrading bacterium from marine sediments*. *Int J Syst Bacteriol* **45**: 116–123.

Eadie, B.J., Landrum, P.F. and Faust, W. (1982).Polycyclic aromatic hydrocarbons in sediments, pore water and the amphipod Pontoporeia hoyi from Lake Michighan. Chemosphere 11, 847-858

Energy Information Administration (EIA) 2016. Offshore oil production in deep water and ultra deep water is increasing. *Today in Energy* October 28, 2016. Retrieved online from https://www.eia.gov/todayinenergy/detail.php?id=28552

Farrell, R.L., Rhodes, P.L., and Aislabie, J. (2003) Toluene degrading Antarctic Pseudomonas strains from fuel contaminated soil. *Biochem. Biophys. Res. Commun* 312: 235–240.

Ferguson DK, Li C., Chakraborty A., Gittins A., Fowler M., Webb J, Campbell C., Morrison N., MacDonald A., Casey R.J. Hubert (2023). Multi-year seabed environmental baseline in deep-sea offshore oil prospective areas established using microbial biodiversity. Marine Pollution Bulletin, Volume 194, Part A, 2023, 115308, https://doi.org/10.1016/j.marpolbul.2023.115308.

Gutierrez, T., Singleton, D.R., Berry, D., Yang, T., Aitken, M.D., and Teske, A. (2013) Hydrocarbon-degrading bacteria enriched by the Deepwater Horizon oil spill identified by cultivation and DNA-SIP. *ISME J*. 7, 2091-2104

Gregson, B.H., Metodieva, G., Metodieva, M., Golyshin, P and McKew B. (2020) Protein expression in the obligate hydrocarbon-degrading psychrophile Oleispira antartica RB-8 during alkane degradation and cold tolerance. Environmental microbiology 22 (5) p 1870-1883.

Hazen, T.C., E.A. Dubinsky, T.Z. DeSantis, G.L. Andersen, Y.M. Piceno, N. Singh, J.K. Jansson, A. Probst, S.E. Borglin, J.L. Fortney, *et al*. 2010. Deep-sea oil plume enriches indigenous oil-degrading bacteria. *Science* 330 (6001): 204- 208 http://dx.doi.org/10.1126/science.1195979.

Head, I. M., D. M. Jones, and W. F. M. Roling. 2006. Marine microorganisms make a meal of oil. *Nat. Rev. Microbiol*. 4:173–182.

Hyne, N.J. (2001). Non-technical Guide to Petroleum Geology, Exploration, Drilling and Production. Tulsa, OK: Penn Well

Joye, S.B., Teske. A.P and Kostka, J.E (2014). Microbial dynamics following the Macondo oil well blowout across Gulf of Mexico environments. BioScience 64(9):766–777, http://dx.doi.org/10.1093/biosci/biu121.

Joye, S.B. (2015). Deepwater Horizon, 5 years on. Science 349(6248):592–593, http://dx.doi.org/10.1126/science.aab4133.

Joye, S.B., S. Kleindienst, J.A. Gilbert, K.M. Handley, P. Weisenhorn, W.A. Overholt, and J.E. Kostka. (2016). Responses of microbial communities to hydrocarbon exposures. *Oceanography* 29 (3):136–149, http://dx.doi.org/10.5670/oceanog.2016.78.

Joye, Samantha B. "The Geology and Biogeochemistry of Hydrocarbon Seeps." *Annual Review of Earth and Planetary Sciences*, vol. 48, no. 1, 2020, pp. 205–31, https://doi.org/10.1146/annurev-earth-063016-020052.

Karickhoff, S., Brown, D. and Scott, T. (1979) Sorption of hydrophobic pollutants on natural sediments. Water Res. 13, 241-248.

Kim, D., Yoo, M., Kim, E., and Hong, S.G. (2013) Anthranilate degradation by a cold-adapted *Pseudomonas sp*. *J Basic Microbiol* 53: 1–9.

Kimes, N.E., Callaghan, A.V., Suflita, J.M., Morris, P.J., (2014). Microbial transformation of the Deepwater Horizon oil spill—past, present, and future perspectives. *Front. Microbiol*. 5 doi: http://dx.doi.org/10.3389/fmicb.2014.00603.

Kosina, M., Bartak, M., Maslanova, I., Pascutti, A.V., Sedo, O., Lexa, M., and Sedlacek, I. (2013). *Pseudomonas prosekii* sp. nov., a novel psychrotrophic bacterium from Antarctica. *Curr Microbiol* 67: 637–646.

Kube, M., Chernikova, T.N., Al-Ramahi, Y., Beloqui, A., Lopez-Cortez, N., Guazzaroni, M.-E., *et al*. (2013) Genome sequence and functional genomic analysis of the oil-degrading bacterium *Oleispira Antarctica*. *Nat Commun* **4**: 2156.

Lam, P., and Kuypers, M.M. (2011) Microbial nitrogen cycling processes in oxygen minimum zones. Ann Rev Mar Sci 3: 317–345.

Lea-Smith, D. J. et al. Contribution of cyanobacterial alkane production to the ocean hydrocarbon cycle. Proc. Natl Acad. Sci. USA 112, 13591–13596 (2015).

Li, Carmen, et al. "Bacterial Anomalies Associated with Deep Sea Hydrocarbon Seepage Along the Scotian Slope." *Deep-Sea Research. Part I, Oceanographic Research Papers*, vol. 193, 2023, p. 103955–, https://doi.org/10.1016/j.dsr.2022.103955.

Love, Connor R., et al. "Microbial Production and Consumption of Hydrocarbons in the Global Ocean." *Nature Microbiology*, vol. 6, no. 4, 2021, pp. 489–98, https://doi.org/10.1038/s41564-020-00859-8.

Martin, Marcel (2011) Cutadapt removes adapter sequences from high-throughput sequencing reads. EMBnet.journal, [S.l.], v. 17, n. 1, p. pp. 10-12, may 2011. ISSN 2226-6089. Available at https://journal.embnet.org/index.php/embnetjournal/article/view/200>. Date accessed: 03 sep. 2022. doi:https://doi.org/10.14806/ej.17.1.200.

Martin Bryan D., Witten Daniela, and. Willis Amy D. (2020) "Modeling microbial abundances and dysbiosis with beta-binomial regression." Ann. Appl. Stat. 14 (1) 94 - 115, March 2020. https://doi.org/10.1214/19-AOAS1283

Mason, O.U., Hazen, T.C., Borglin, S., Chain, P.S.G., Dubinsky, E.A., Fortney, J.L., *et al*. (2012) Metagenome, metatranscriptome and single-cell sequencing reveal microbial response to Deepwater horizon oil spill. *ISME J* **6**: 1715– 1727.

McGroddy, S.E., and Farrington, J.W. (1995) Sediment porewater partitioning of polycyclic aromatic hydrocarbon in three cores from Boston harbor, Massachusetts. *Environ. Sci. Technol*. 29, 1542 – 50

Normandeau, A., Campbell, D.C., 2020. Recurrence of turbidity currents on glaciated continental margins: A conceptual model from eastern Canada. J. Sediment. Res. 90, 1305–1321.

Novotnik B, Zorz J, Bryant S and Strous M (2019) The Effect of Dissimilatory Manganese Reduction on Lactate Fermentation and Microbial Community Assembly. Front. Microbiol. 10:1007. doi: 10.3389/fmicb.2019.01007

Offshore Technology (OT) 2017. Carcara Discovery, Santos Basin. February 3rd, 2017. Retrived online from https://www.offshore-technology.com/projects/carcara-discovery-santos-basin/

Passow, U., Ziervogel, K., Asper, V., Diercks, a., 2012. Marine snow formation in the aftermath of the Deepwater Horizon oil spill in the Gulf of Mexico. Environ. Res. Lett. 7 (3). http://dx.doi.org/10.1088/1748-9326/7/3/035301 (035301).

Prince, R.C., and Suflita, J.M. (2007) Anaerobic biodegradation of natural gas condensate can be stimulated by the addition of gasoline. *Biodegradation* 18:515–523. doi 10.1007/s10532-006-9084-4

Pruesse Elmar, Jörg Peplies, Frank Oliver Glöckner, SINA: Accurate high-throughput multiple sequence alignment of ribosomal RNA genes (2012) *Bioinformatics*, Volume 28, Issue 14, Pages 1823–1829, https://doi.org/10.1093/bioinformatics/bts252

Radwan, S, Khanafer M., and Al-Awadhi A. (2019) Ability of the So-Called Obligate Hydrocarbonoclastic Bacteria to Utilize Nonhydrocarbon Substrates Thus Enhancing Their

651 Activities Despite Their Misleading Name. *BMC Microbiology*, vol. 19, no. 1, 2019, pp. 41–41,
652 https://doi.org/10.1186/s12866-019-1406-x.

653

654 Redmond, M.C., and Valentine, D.L., 2012. Natural gas and temperature structured a microbial
655 community response to the Deepwater Horizon oil spill. Proc. Natl. Acad. Sci. 109 (50), pp
656 20292-20297 doi: http://dx.doi.org/10.1073/pnas.1108756108.

657

658 Sanni, G.O., Coulon, F., and McGenity, T.J. (2015) Dynamics and distribution of bacterial and
659 archaeal communities in oil-contaminated temperate coastal mudflat mesocosms. Environ. Sci.
660 Pollut. Res. 22, 15230-15247. Doi:10.1007/s11356-015-4313-1.

661

662 Shukla, A and Karki H. (2016) Applications of robotics in offshore oil and gas industry- A
663 review Part II. Robotics and autonomous systems, Vol. 75, p. 508 – 524.

664

665 Stamatakis Alexandros, RAxML version 8: a tool for phylogenetic analysis and post-analysis of
666 large phylogenies, *Bioinformatics*, Volume 30, Issue 9, May 2014, Pages 1312–
667 1313, https://doi.org/10.1093/bioinformatics/btu033

668

669 Takahashi, S., Tomita, J., Nishioka, K., Hisada, T., and Nishijima, M. (2014) Development of a
670 Prokaryotic Universal Primer for Simultaneous Analysis of Bacteria and Archaea Using Next-
671 Generation Sequencing. PLoS ONE 9(8): e105592. doi:10.1371/journal.pone.0105592

672

673 Tan BoonFei, Kathleen Semple, Julia Foght (2015) Anaerobic alkane biodegradation by cultures
674 enriched from oil sands tailings ponds involves multiple species capable of fumarate
675 addition, *FEMS Microbiology Ecology*, 91 (5): https://doi-
676 org.ezproxy.lib.ucalgary.ca/10.1093/femsec/fiv042

677

678 Townsend GT Prince RC Suflita JM Anaerobic biodegradation of alicyclic constitutents of
679 gasoline and natural gas condensate by bacteria from an anoxic aquifer *FEMS Microbiol Ecol*
680 2004 49 129 35
681

682 Valentine, D.L., Fisher, G.B., Bagby, S.C., Nelson, R.K., Reddy, C.M., Sylva, S.P., Woo, M. A.,
683 2014. Fallout plume of submerged oil from Deepwater Horizon. Proc. Natl. Acad. Sci. U. S. A.
684 111 (45), 15906–15911. doi:http://dx.doi.org/10.1073/ pnas.1414873111.

685

Whyte, L.G., Bourbonniere, L., and Greer, C.W. (1997). Biodegradation of petroleum hydrocarbons by psychrotrophic *Pseudomonas* strains possessing both alkane (alk) and naphthalene (nah) catabolic pathways. Appl Environ Microbiol 63 (9): 3719-3723

Wickham, H. (2016). *Ggplot2: Elegant graphics for data analysis* (2nd ed.) [PDF]. Springer International Publishing.

Willis, A. D. and Martin, B. D. (2022) Estimating diversity in networked ecological communities, *Biostatistics*, Volume 23, Issue 1, January 2022, P. 207-222, https://doi.org/10.1093/biostatistics/kxaa015

Yakimov, M.M., Golyshin, P.N., Lang, S., Moore, E.R., Abraham, W.R., Lünsdorf, H., and Timmis, K.N. (1998) *Alcanivorax borkumensis* gen. Nov., sp. nov., a new, hydrocarbon-degrading and surfactant-producing marine bacterium. *Int J Syst Bacteriol* **48**: 339– 348.

Yakimov, M.M., Timmis, K.N., and Golyshin, P.N. (2007). Obligate oil-degrading marine bacteria. *Curr Opin Biotechnol* 18: 257–266.

Yakimov, M.M., Giuliano, L., Gentile, G., Crisafi, E., Chernikova, T.N., Abraham, W.-R., *et al*. (2003) *Oleispira antarctica* gen. nov., sp. nov., a novel hydrocarbonoclastic marine bacterium isolated from Antarctic coastal sea water. *Int J Syst Evol Microbiol* **53**: 779– 785.

Yakimov, M.M., Giuliano, L., Denaro, R., Crisafi, E., Chernikova, T.N., Abraham, W.-R., *et al*. (2004) *Thalassolituus oleivorans* gen. Nov., sp. nov., a novel marine bacterium that obligately utilizes hydrocarbons. *Int J Syst Evol Microbiol* **54**: 141– 148.

Yang,T., Nigro, L.M., Gutierrez,T., D'Ambrosio, L., Joye,S.B., Highsmith,R., Teske,A. P., 2016. Pulsed blooms and persistent oil-degrading bacteria in the water column during and after the Deep -Water Horizon blowout. Deep Sea Res.II: 129, 282–291. http://dx.doi.org/10.1016/j.dsr2.2014.01.014.

Yasuhara, M. and Danovaro, R. (2016). Temperature impacts on deep-sea biodiversity. Biological reviews of the Cambridge Philosophical Society, Vol.91 (2), p.275-287

Yergeau, E., Sanschagrin, S., Beaumier, D., and Greer, C.W. (2012). Metagenomic analysis of the bioremediation of diesel-contaminated Canadian high arctic soils. *PLoS ONE* 7: e30058

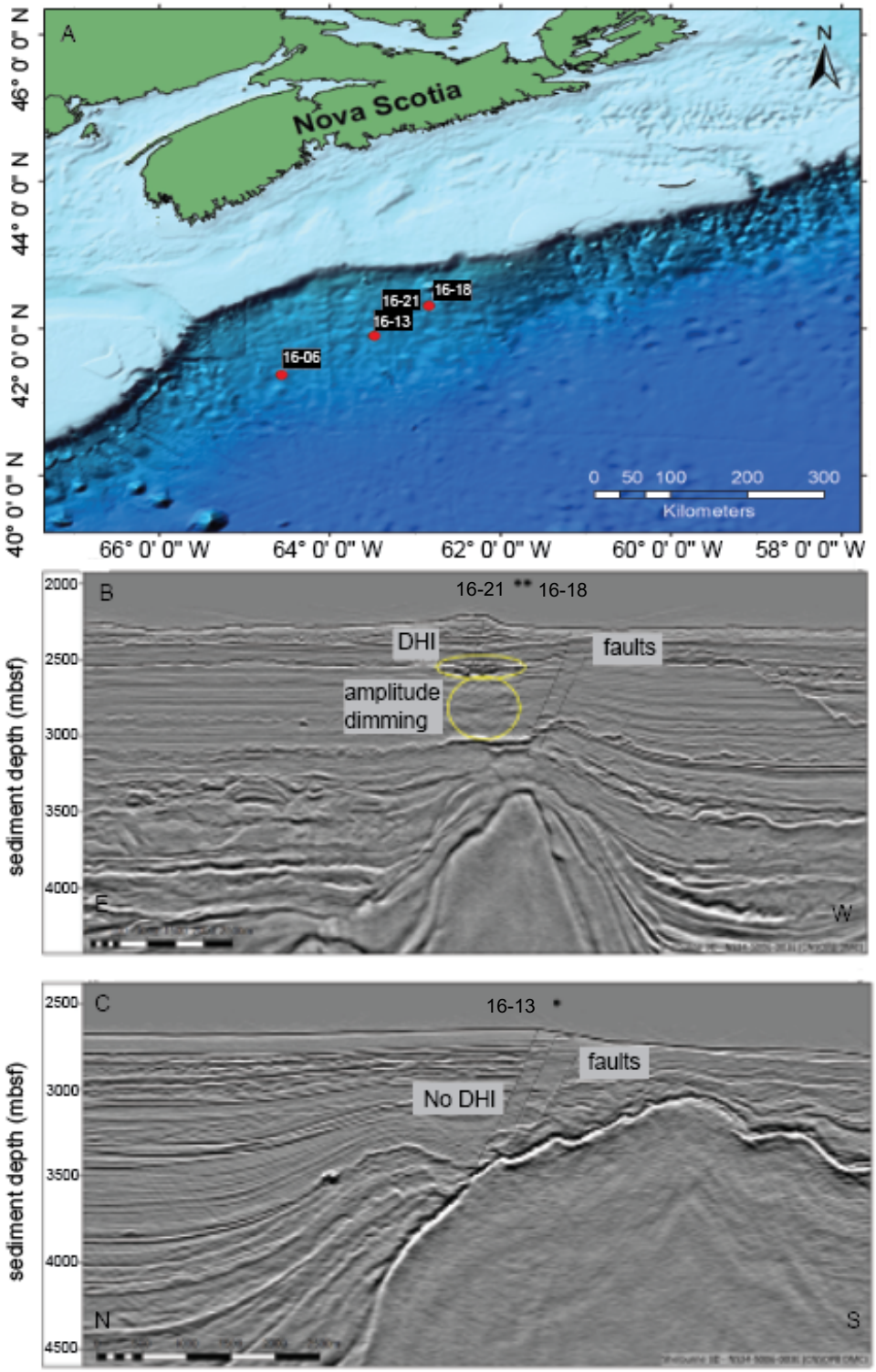

Figure 1: Map of the Scotian Slope, NW Atlantic Ocean showing (A) the location of four piston coring sites sampled aboard CCGS *Hudson* in 2016. Sites 16-18 and 16-21 are 160m apart and overlap on the map. Geophysical images showing sites 16-18 and 16-21 (B) and site 16-13 (C) at higher resolution reveal suspected direct hydrocarbon indicators (DHIs) such as deep-seated fault near surface, amplitude diming (in circles) and faults (broken lines) for sites 16-18 and 16-21, but not 16-13 which shows only faults to surface above a large shallow diapir.

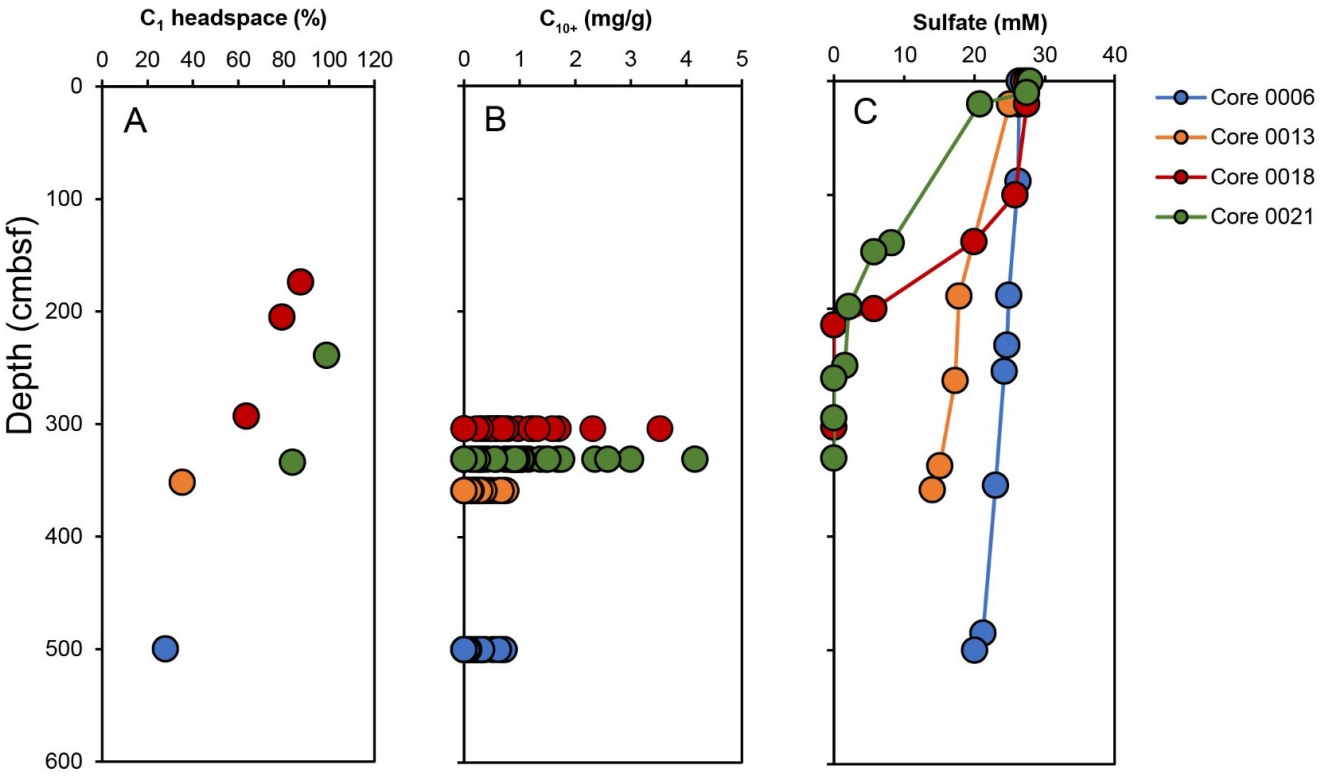

Figure 2: Sediment geochemical parameters in four sediment cores. (A) C_1 gas measurements made following incubating different sediment depths in isojars immediately after sampling. (B) Liquid hydrocarbons were assessed using GC-MS for sediment sampled from the bottom of each of the cores, with each symbol of the same colour denoting different individual compounds in the C_{10} to C_{42} range. (C) Porewater sulfate concentrations determined at different depths throughout each core.

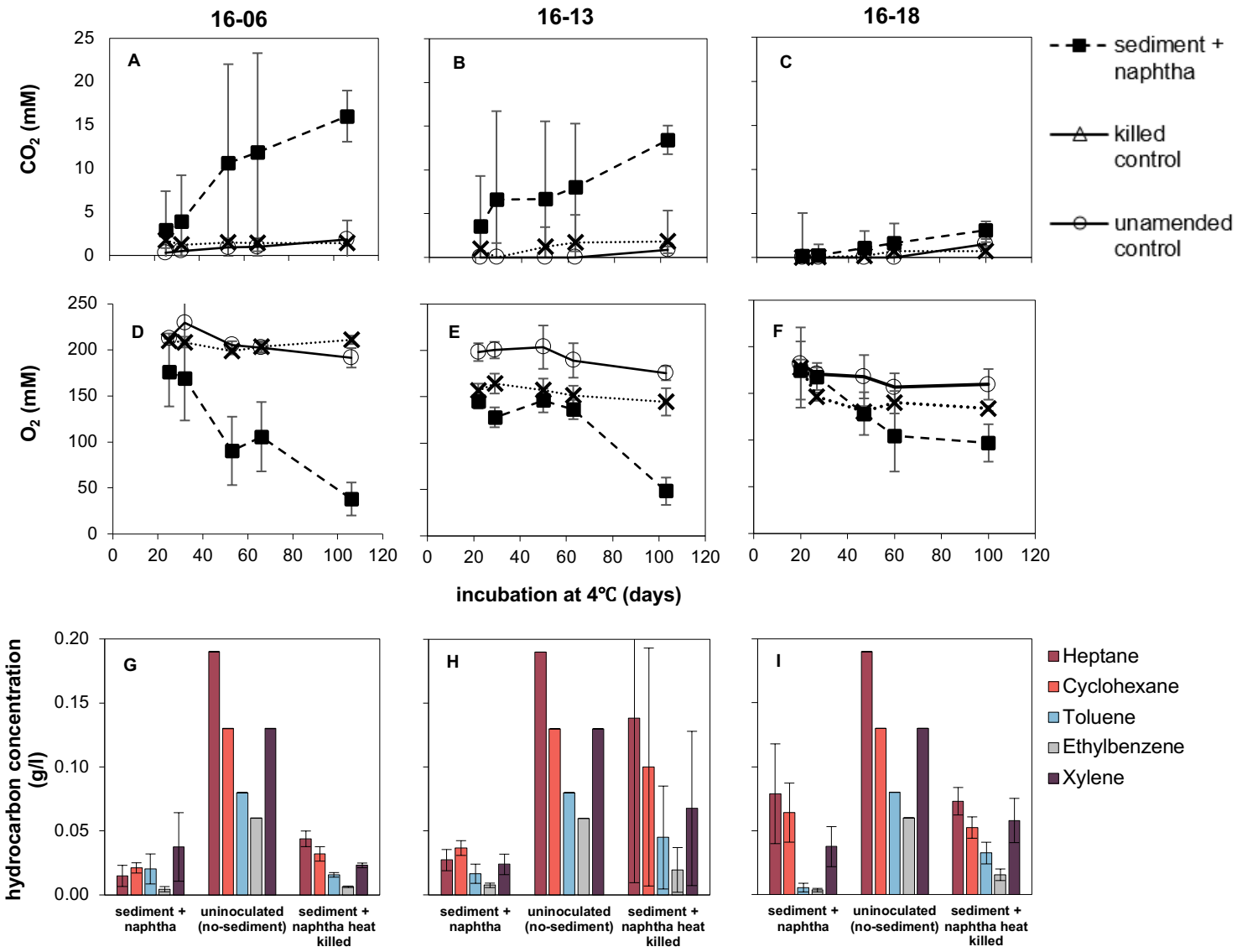

Figure 3: Analysis of carbon dioxide (A-C), oxygen (D-F) and volatile hydrocarbons (G-I) in the headspace of surface sediment (0-20 cmbsf) microcosms during incubation at 4°C. Carbon dioxide production (A-C) and oxygen consumption (D-F) over time reveal most activity during the first 100 days of incubation. Analysis of headspace hydrocarbons after 100 days (G-I) show much lower hydrocarbon concentrations in microcosms that combined sediment and naphtha, compared to uninoculated sediment-free controls (the same data for these controls are plotted beside each of the three sediment-inoculate microcosms in G-I to enable easier comparison). Hydrocarbon concentrations were calculated relative to composition of specific compound in naphtha added.

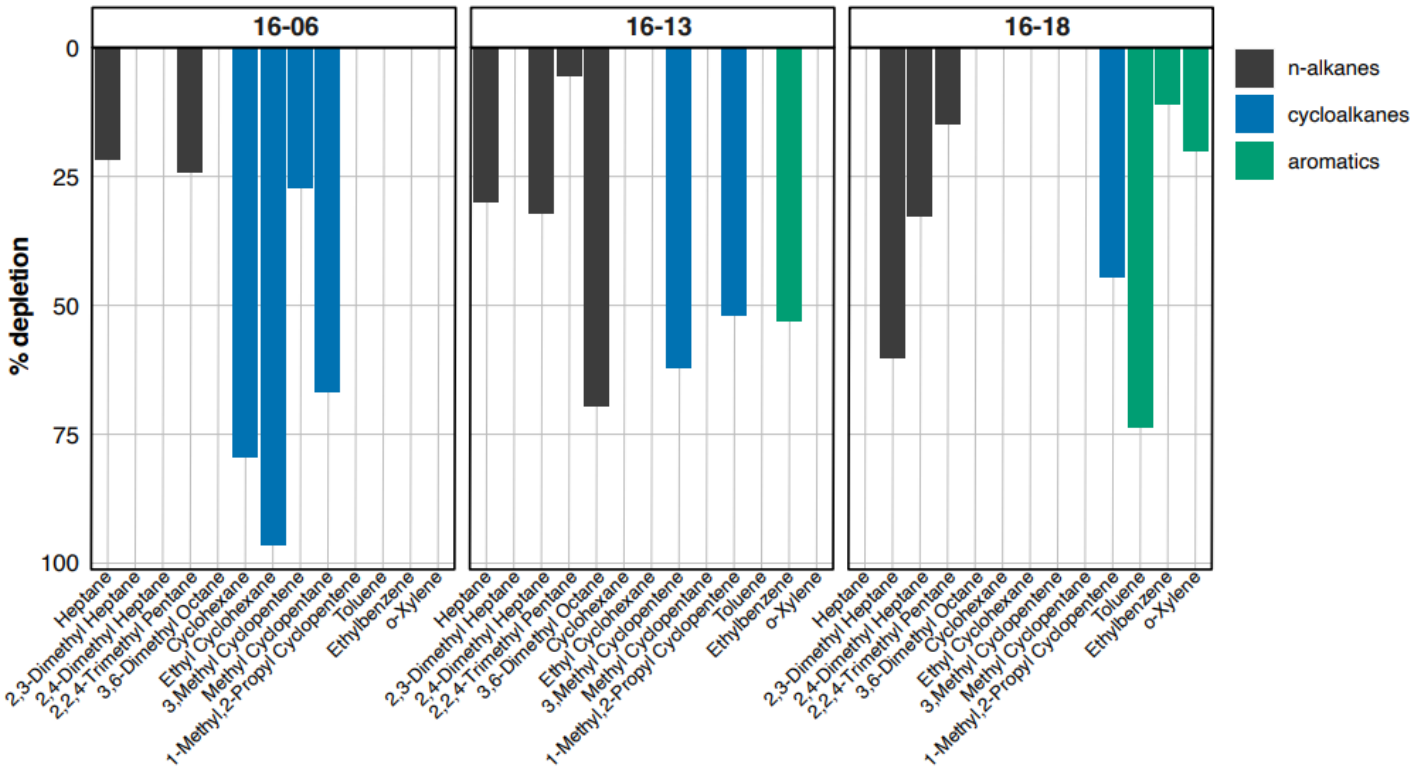

Figure 4: Percentage headspace hydrocarbon depleted in naphtha-amended sediment microcosms relative to heat killed controls for the same sediments between 50 and 100 days of incubation at 4°C.

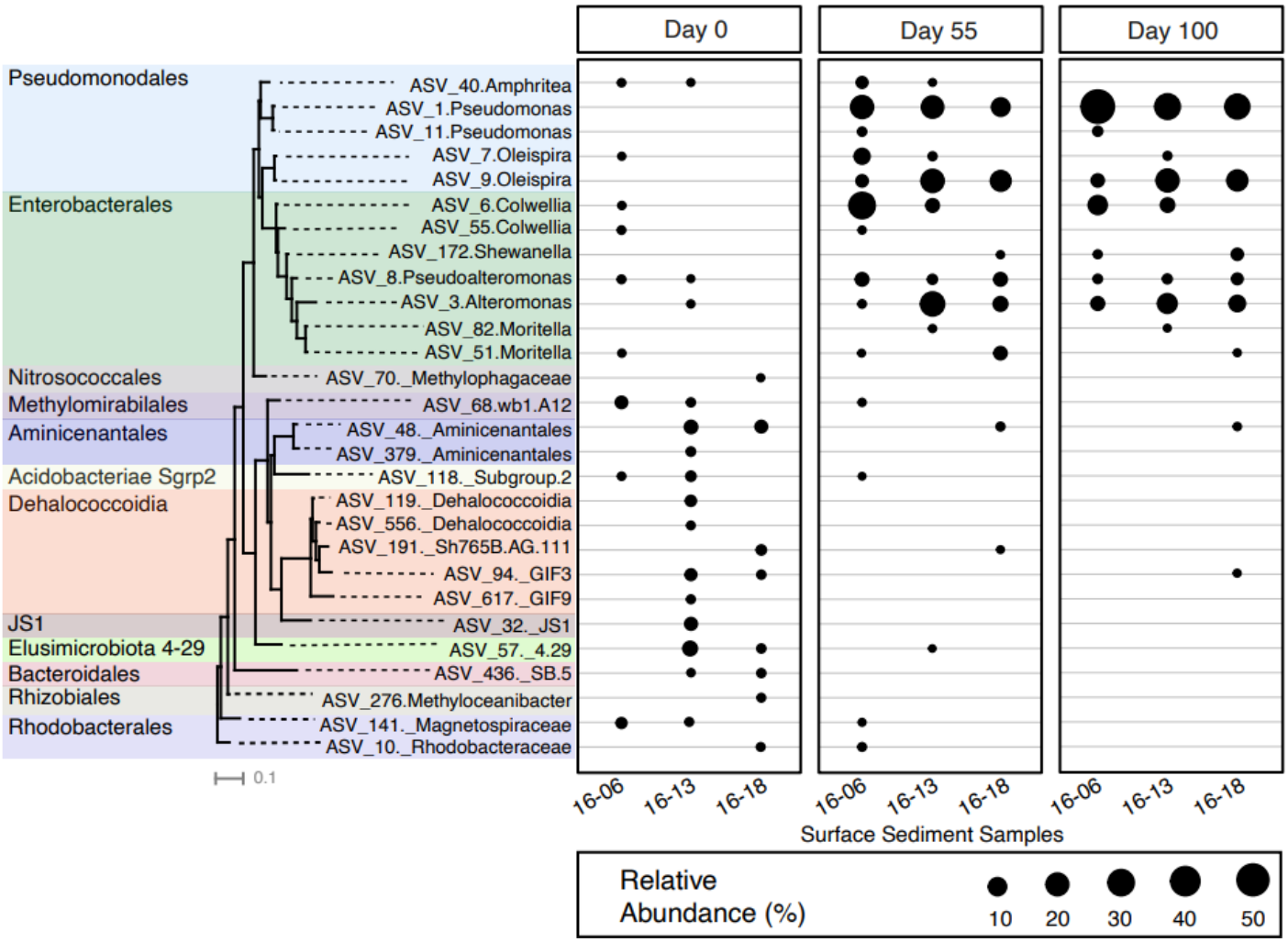

Figure 5: Relative sequence abundance of significantly enriched ASVs in naphtha-amended microcosms over 100 days at 4°C revealed by differential abundance analysis of 16S rRNA gene amplicon libraries. The extra underscore indicates a taxonomy classification at a level higher than genus.

Table 1: Site location and core information of sampled cores[1] from the Scotian slope, NW Atlantic Ocean

Core	Coordinates	Water depth (m)	Surface sediment for microcosm establishment	Subsurface sediment for microcosm establishment	Hydrocarbon assessment
16-06	41º37.4476N 64º56.3773W	3260	0-20 cmbsf	Not sampled	No faults No acoustic DHIs
16-13	41º90.5008N 63º47.7986W	2601	0-20 cmbsf	Not sampled	Faults No acoustic DHIs
16-18	42º30.8748N 62º83.6243W	2235	0-20 cmbsf	134-141 cmbsf	Faults Acoustic DHIs
16-21	42º30.8531N 62º83.8306W	2930	Not sampled	142-148 cmbsf	Faults Acoustic DHIs

[1] All sampling was conducted during the summer in 2016.

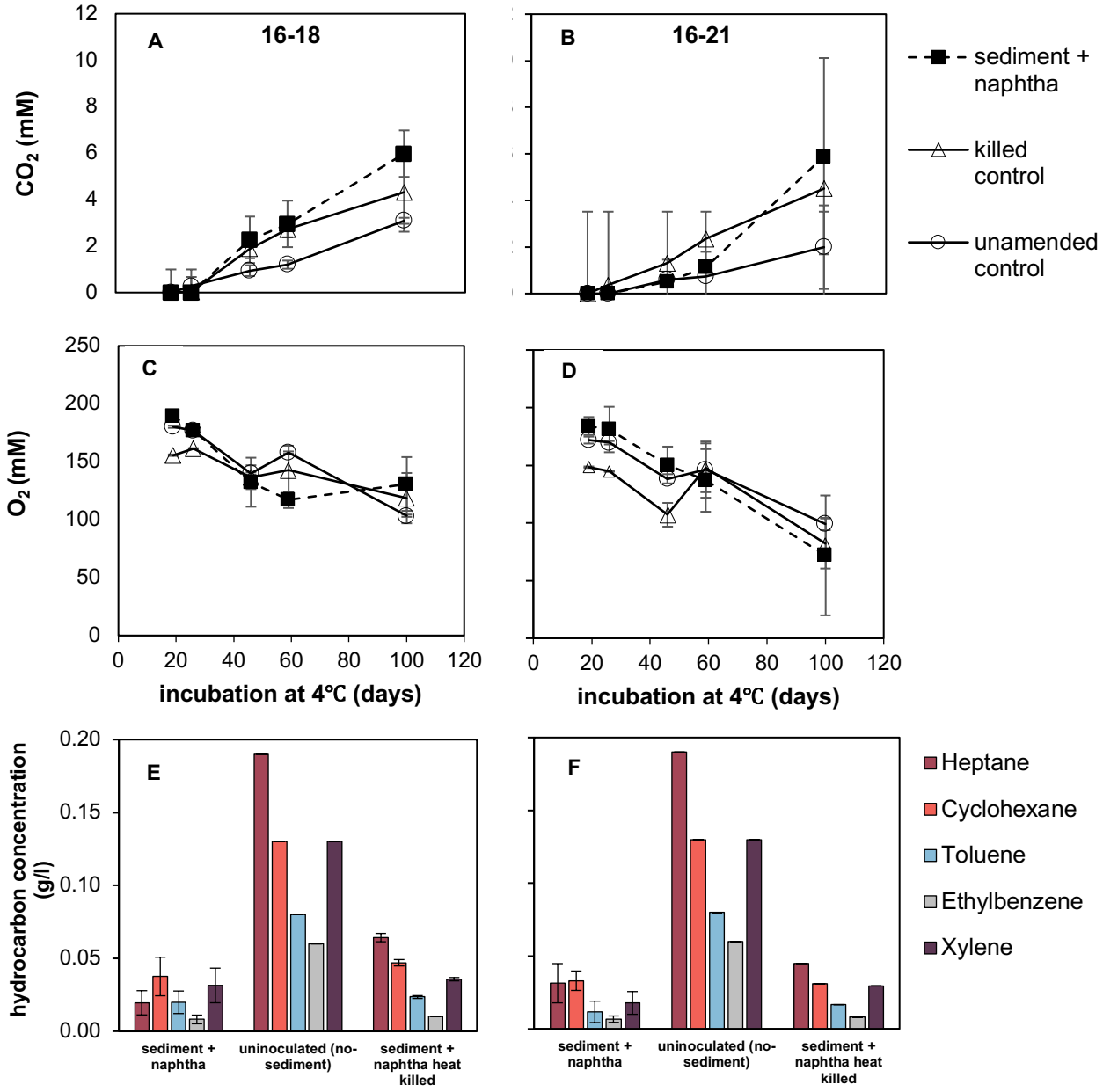

Figure S1: Analysis of carbon dioxide (A, B), oxygen (C, D) and volatile hydrocarbons (E, F) in the headspace of deeper sediment 16-18 (134-141 cmbsf), 16-21 (142-148 cmbsf) microcosms during incubation at 4°C. Carbon dioxide production (A, B) over time reveal most activity during the first 100 days of incubation. Analysis of headspace hydrocarbons after 100 days (E, F) show much lower hydrocarbon concentrations in microcosms that combined sediment and naphtha, compared to uninoculated sediment-free controls (the same data for these controls are plotted beside each of the two sediment-inoculate microcosms in E & F to enable easier comparison). Hydrocarbon concentrations were calculated relative to composition of specific compound in naphtha added.

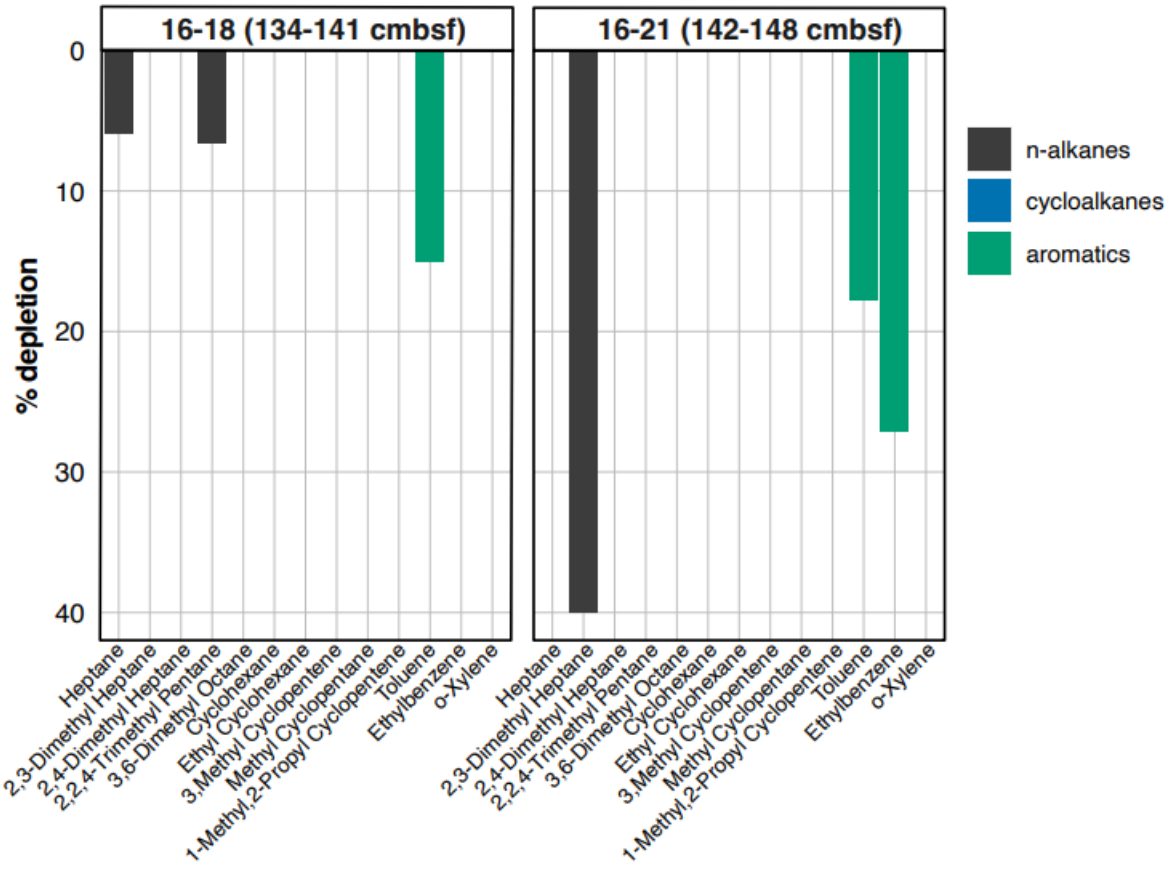

Figure S2: Percentage headspace hydrocarbon depleted in naphtha amended subsurface sediment microcosms relative to heat killed controls for the same sediments between 50 and 100 days of incubation at 4°C.

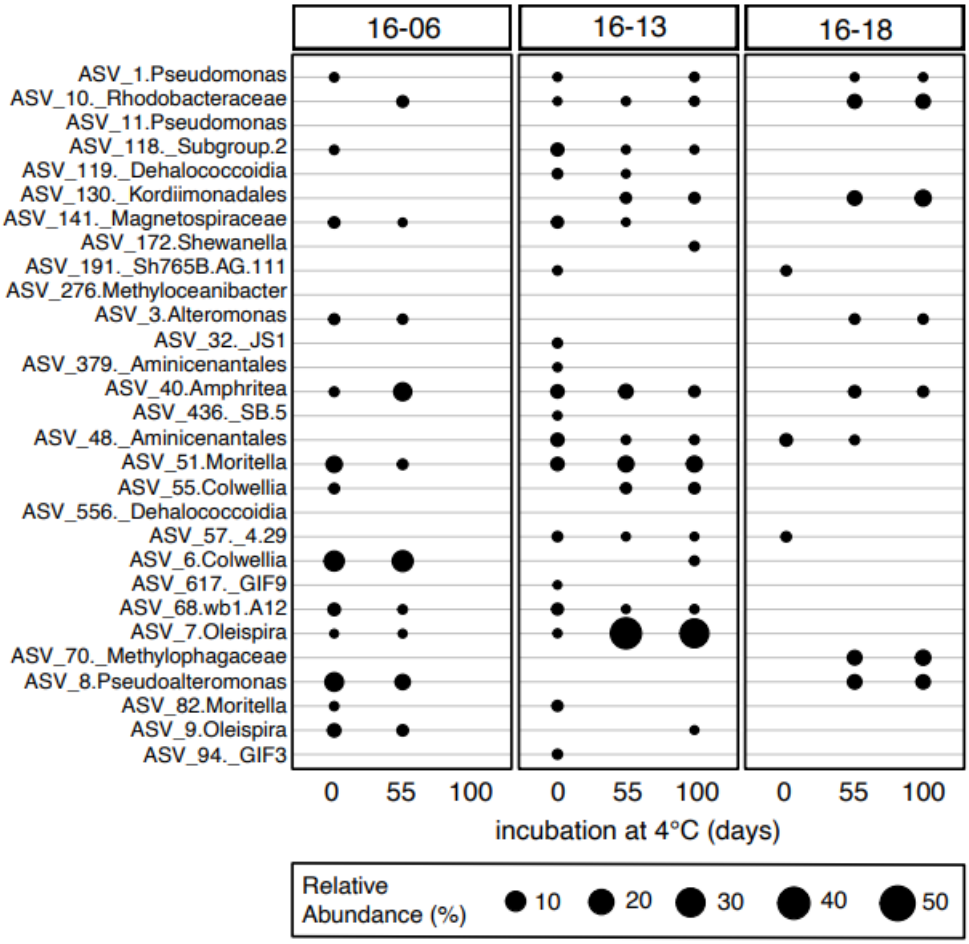

Figure S3: Relative sequence abundance of statistically significant ASVs revealed by differential analysis based on 16S rRNA gene amplicons showing community change in unamended microcosms inoculated with surface sediment during a period of 100 days incubation at 4°C. The extra underscore indicates a taxonomy classification at a level higher than genus.

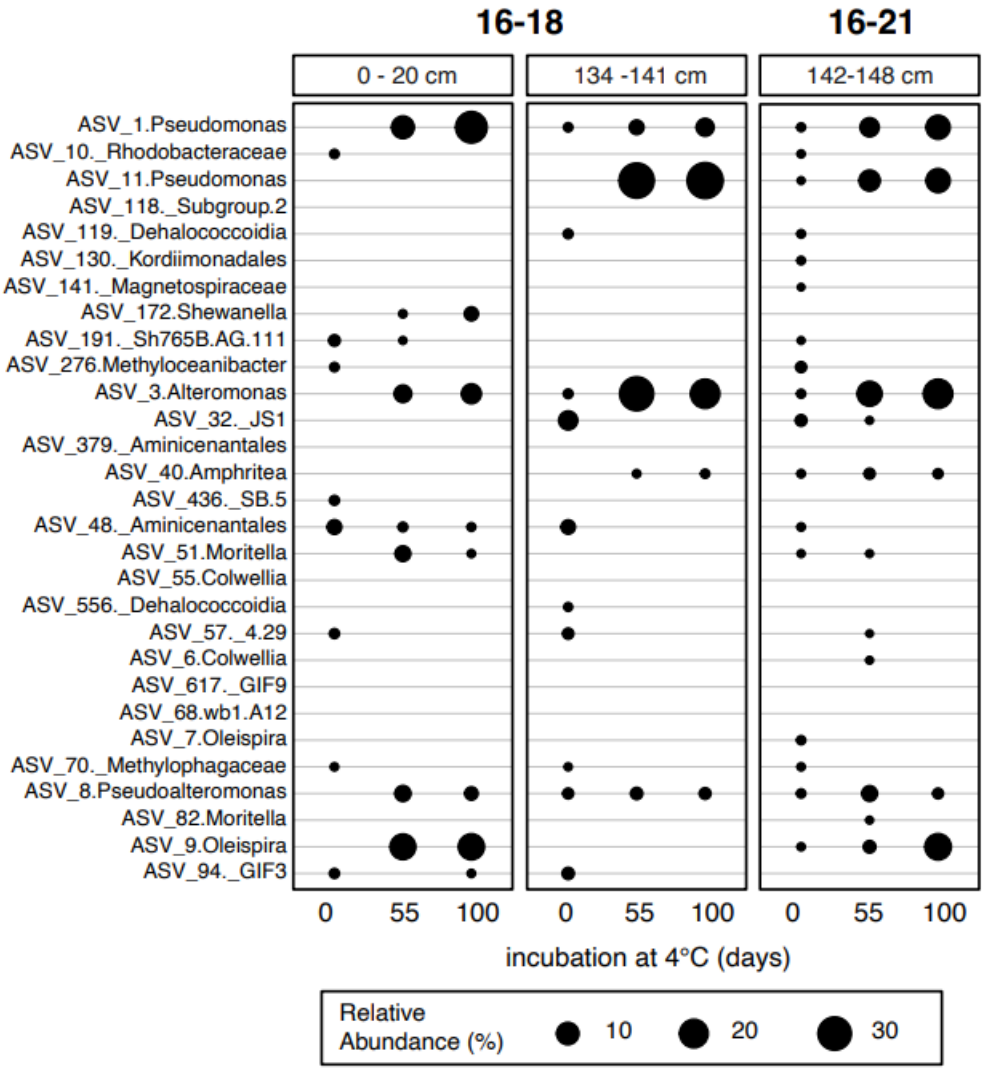

Figure S4: Relative sequence abundance of statistically significant ASVs revealed by differential analysis based on 16S rRNA gene amplicons showing community change in naphtha-amended microcosms inoculated with surface and deeper sediment (16-18) and deeper sediment (16-21) during a period of 100 days incubation at 4°C. The extra underscore indicates a taxonomy classification at a level higher than genus.

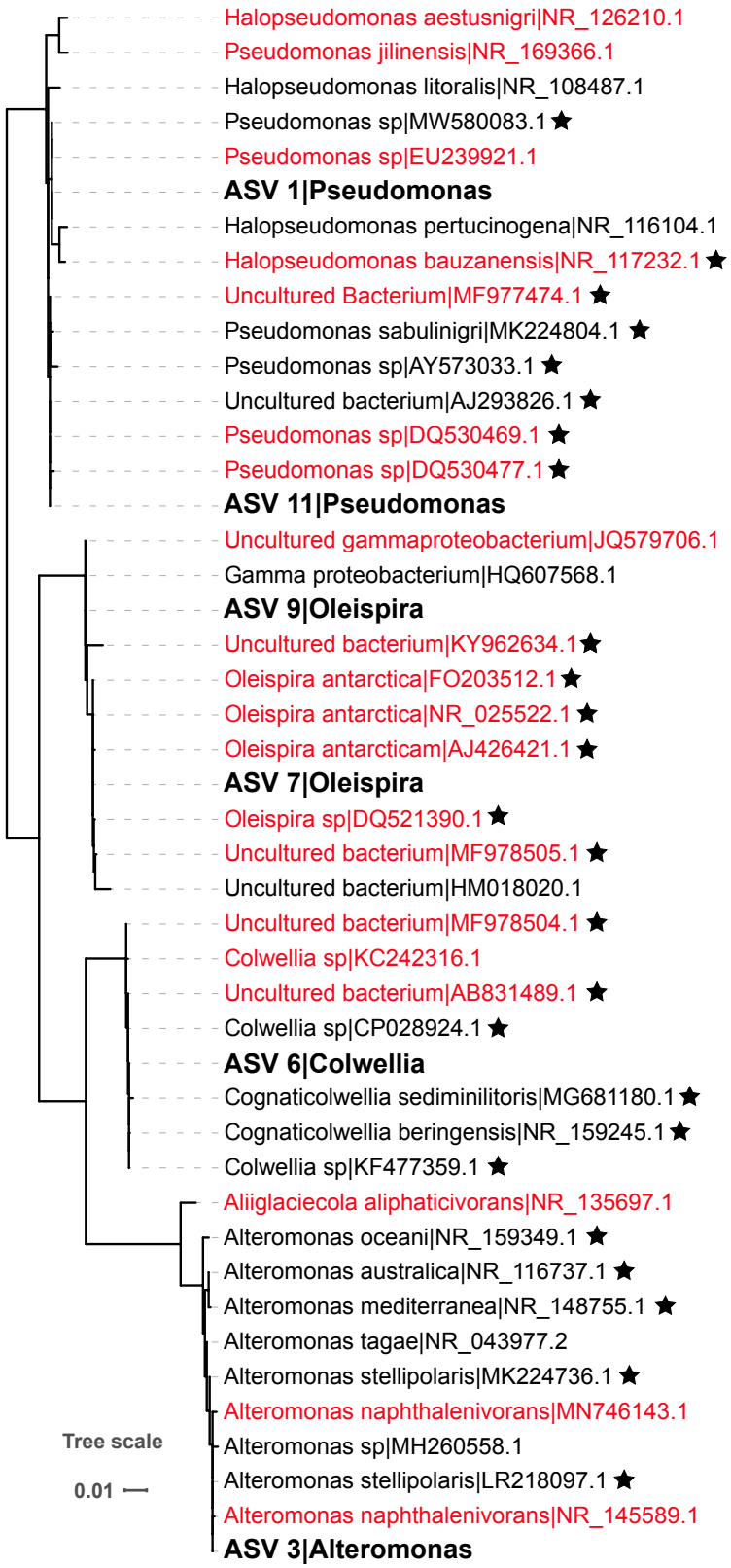

Figure S5: Phylogeny of ASVs from sediment incubations (bold) affiliated with known hydrocarbon-degrading genera and their close sequence matches (≥99% sequence identity) in the NCBI nr database. NCBI hits annotated as being from hydrocarbon-associated environments are highlighted in red, and hits with cold tolerance as demonstrated through their cultivation or inferred from the environment are marked by a star.

Table S1. Analysis of variance (ANOVA) comparing respiration in naphtha amendment, heat killed and unamended microcosms of each tested core.

Core	Day		Sum Sq	Mean Sq	F Val	Probability
16 - 06 (0-20cm)	20	O_2	2531	1265.5	26.67	0.15
	60		25039	12520	26.63	1.04 e-03**
	100		53808	26904	177	6e-06***
	20	CO_2	31.6	15.80	2.32	0.18
	60		530.0	265.02	6.16	0.0351*
	100		1080.3	540.2	186.7	3.96e-06***
16 - 13 (0-20cm)	20	O_2	5483	2742	1.933	0.225
	60		5182	2591	1.786	0.246
	100		30758	15379	35.29	4.81 e-04***
	20	CO_2	23.86	11.93	0.933	0.444
	60		124.0	61.98	2.996	0.125
	100		370.6	185.31	178.6	4.51e-06***
16 - 18 (0-20cm)	20	O_2	79	39.6	0.042	0.959
	60		4320	2159.8	3.58	0.0948
	100		5971	2985.6	13.18	6.38 e-03**
	20	CO_2	0.0857	0.0428	0.99	0.422
	60		4.141	2.071	1.276	0.345
	100		8.749	4.375	12.5	7.25 e-03**
16 - 18 (134-141cm)	20	O_2	1231.2	615.6	84.63	0.0023**
	60		1692	845.8	2.323	0.246
	100		750.5	375.5	1.085	0.442
	20	CO_2	NA	NA	NA	NA
	60		3.622	1.8112	4.113	0.138
	100		8.401	4.201	2.612	0.22
16 - 21 (142-148 cm)	20	O_2	1532	766	16.93	0.0112*
	60		179.9	90	0.243	0.795
	100		892	445.9	0.322	0.742
	20	CO_2	NA	NA	NA	NA
	60		2.858	1.429	5.067	0.080
	100		18.34	9.170	1.716	0.29

Sum Sq: Sum of squares; Mean Sq: Mean sum of squares.

F val: F value; Signif. codes: *** P 0.001 ** P 0.01 * P 0.05

NA: Not applicable as all values were 0.

Table S2. Analysis of variance (ANOVA) comparing hydrocarbon concentration in naphtha amendment, heat killed and unamended microcosms of each tested core after 100 days of incubation at 4℃.

Core	Hydrocarbon	Sum Sq	Mean Sq	F Val	Probability
16 - 06 (0-20cm)	Heptane	0.02	0.01	221.19	8.03 e -05***
	Cyclohexane	0.001	0.005	195.59	1.02 e-04***
	Toluene	0.003	0.001	23.61	6.09 e-03**
	Ethylbenzene	0.003	0.001	570.67	1.22 e-05***
	Xylene	0.02	0.01	41.99	0.02*
16 - 13 (0-20cm)	Heptane	0.03	0.01	1.70	0.29
	Cyclohexane	0.01	0.004	1.07	0.42
	Toluene	0.003	0.002	1.95	0.26
	Ethylbenzene	0.002	0.001	6.69	0.05*
	Xylene	0.009	0.004	2.41	0.2
16 - 18 (0-20cm)	Heptane	0.01	0.006	0.79	0.51
	Cyclohexane	0.005	0.002	0.89	0.47
	Toluene	0.004	0.002	6.51	0.06
	Ethylbenzene	0.002	0.001	12.87	0.02*
	Xylene	0.006	0.003	1.41	0.34
16 - 18 (134-141cm)	Heptane	0.019	0.009	252.93	3.93 e-03**
	Cyclohexane	0.006	0.003	34.79	0.03*
	Toluene	0.003	0.001	45.12	0.02*
	Ethylbenzene	0.002	0.001	231.05	4.30 e-03**
	Xylene	0.007	0.004	52.68	0.02*
16 - 21 (142-148 cm)	Heptane	0.019	0.009	53.53	0.02*
	Cyclohexane	0.008	0.004	85.61	0.01*
	Toluene	0.004	0.002	33.37	0.03*
	Ethylbenzene	0.002	0.001	230.98	4.31 e-03**
	Xylene	0.009	0.005	79.09	0.01*

Sum Sq: Sum of squares; Mean Sq: Mean sum of squares.

F val: F value; Signif. codes: *** P 0.001 ** P 0.01 * P 0.05

Table S3. Description and read count for 16S rRNA gene amplicon libraries.

Library	Core	Treatment	Core Section	Time	Rep	Reads-Raw	Reads-Filtered
13_PC_BS_0cm_TBS_1	16-13	in situ	0cm	TBS	1	68913	28554
13_PC_BS_0cm_TBS_2	16-13	in situ	0cm	TBS	2	28013	13378
13_PC_BS_0cm_TBS_3	16-13	in situ	0cm	TBS	3	16197	6778
13_PC_BS_20cm_TBS_1	16-13	in situ	20cm	TBS	1	37582	14580
13_PC_BS_20cm_TBS_2	16-13	in situ	20cm	TBS	2	25532	12436
13_PC_BS_20cm_TBS_3	16-13	in situ	20cm	TBS	3	8901	3415
13_PC_NA_OX_T0_1	16-13	Naphtha	0-20	Day 0	1	63427	31508
13_PC_NA_OX_T0_2	16-13	Naphtha	0-20	Day 0	2	50127	24589
13_PC_NA_OX_T0_3	16-13	Naphtha	0-20	Day 0	3	120670	58376
13_PC_NA_OX_T1_1	16-13	Naphtha	0-20	Day 50	1	100964	53304
13_PC_NA_OX_T1_2	16-13	Naphtha	0-20	Day 50	2	84322	56213
13_PC_NA_OX_T1_3	16-13	Naphtha	0-20	Day 50	3	28467	14538
13_PC_NA_OX_T2_1	16-13	Naphtha	0-20	Day 100	1	26350	13251
13_PC_NA_OX_T2_2	16-13	Naphtha	0-20	Day 100	2	70306	47777
13_PC_NA_OX_T2_3	16-13	Naphtha	0-20	Day 100	3	67189	34131
13_PC_UN_OX_T0_3	16-13	Naphtha	0-20	Day 0	3	77685	35965
13_PC_UN_OX_T1_3	16-13	Naphtha	0-20	Day 50	3	49951	28427
13_PC_UN_OX_T2_3	16-13	Naphtha	0-20	Day 100	3	90644	53020
18_PC_NA_AN_T0_1	16-18	Naphtha	134-141	Day 0	1	102873	21871
18_PC_NA_AN_T0_2	16-18	Naphtha	134-141	Day 0	2	37588	5618
18_PC_NA_AN_T1_1	16-18	Naphtha	134-141	Day 50	1	52960	12134
18_PC_NA_AN_T1_2	16-18	Naphtha	134-141	Day 50	2	55584	11068
18_PC_NA_AN_T2_1	16-18	Naphtha	134-141	Day 100	1	61778	12414
18_PC_NA_AN_T2_2	16-18	Naphtha	134-141	Day 100	2	48266	11159
18_PC_NA_OX_T0_1	16-18	Naphtha	0-20	Day 0	1	53631	9050

18_PC_NA_OX_T0_2	16-18	Naphtha	0-20	Day 0	2	126587	24111
18_PC_NA_OX_T0_3	16-18	Naphtha	0-20	Day 0	3	45988	7220
18_PC_NA_OX_T1_1	16-18	Naphtha	0-20	Day 50	1	59846	12285
18_PC_NA_OX_T1_2	16-18	Naphtha	0-20	Day 50	2	73274	9275
18_PC_NA_OX_T1_3	16-18	Naphtha	0-20	Day 50	3	80382	17898
18_PC_NA_OX_T2_1	16-18	Naphtha	0-20	Day 100	1	46501	10074
18_PC_NA_OX_T2_2	16-18	Naphtha	0-20	Day 100	2	37888	7957
18_PC_NA_OX_T2_3	16-18	Naphtha	0-20	Day 100	3	48739	8717
18_PC_UN_OX_T0_3	16-18	Unamended	0-20	Day 0	3	42398	8059
18_PC_UN_OX_T1_3	16-18	Unamended	0-20	Day 50	3	63664	15785
18_PC_UN_OX_T2_3	16-18	Unamended	0-20	Day 100	3	84820	22177
21_PC_NA_AN_T0_1	16-21	Naphtha	142-148	Day 0	1	542925	245687
21_PC_NA_AN_T0_2	16-21	Naphtha	142-148	Day 0	2	53654	24015
21_PC_NA_AN_T0_3	16-21	Naphtha	142-148	Day 0	3	74551	32453
21_PC_NA_AN_T1_1	16-21	Naphtha	142-148	Day 50	1	111523	52267
21_PC_NA_AN_T1_2	16-21	Naphtha	142-148	Day 50	2	85445	35070
21_PC_NA_AN_T1_3	16-21	Naphtha	142-148	Day 50	3	99668	43013
21_PC_NA_AN_T2_1	16-21	Naphtha	142-148	Day 100	1	87234	38298
21_PC_NA_AN_T2_2	16-21	Naphtha	142-148	Day 100	2	105263	43592
21_PC_NA_AN_T2_3	16-21	Naphtha	142-148	Day 100	3	63234	26824
21_PC_UN_AN_T0_1	16-21	Unamended	142-148	Day 0	1	1104	145
21_PC_UN_AN_T0_2	16-21	Unamended	142-148	Day 0	2	52026	23598
21_PC_UN_AN_T1_1	16-21	Unamended	142-148	Day 50	1	116479	54463
21_PC_UN_AN_T1_2	16-21	Unamended	142-148	Day 50	2	82790	36920
21_PC_UN_AN_T2_1	16-21	Unamended	142-148	Day 100	1	27585	10381
21_PC_UN_AN_T2_2	16-21	Unamended	142-148	Day 100	2	73325	29910

6_PC_BS_0cm_TBS_1	16-06	in situ	0cm	TBS	1	107353	37578
6_PC_BS_0cm_TBS_2	16-06	in situ	0cm	TBS	2	86573	31704
6_PC_BS_0cm_TBS_3	16-06	in situ	0cm	TBS	3	68553	25839
6_PC_BS_20cm_TBS_1	16-06	in situ	20cm	TBS	1	61646	21459
6_PC_BS_20cm_TBS_2	16-06	in situ	20cm	TBS	2	102366	38911
6_PC_BS_20cm_TBS_3	16-06	in situ	20cm	TBS	3	56663	19880
6_PC_NA_OX_T0_1	16-06	Naphtha	0-20	Day 0	1	56220	24682
6_PC_NA_OX_T0_2	16-06	Naphtha	0-20	Day 0	2	52597	22262
6_PC_NA_OX_T0_3	16-06	Naphtha	0-20	Day 0	3	103443	42542
6_PC_NA_OX_T1_1	16-06	Naphtha	0-20	Day 50	1	99888	56890
6_PC_NA_OX_T1_2	16-06	Naphtha	0-20	Day 50	2	96378	55388
6_PC_NA_OX_T1_3	16-06	Naphtha	0-20	Day 50	3	54027	29668
6_PC_NA_OX_T2_1	16-06	Naphtha	0-20	Day 100	1	44976	23396
6_PC_NA_OX_T2_2	16-06	Naphtha	0-20	Day 100	2	67414	33963
6_PC_NA_OX_T2_3	16-06	Naphtha	0-20	Day 100	3	51115	25481
6_PC_UN_OX_T0_3	16-06	Unamended	0-20	Day 0	3	102921	47855
6_PC_UN_OX_T1_3	16-06	Unamended	0-20	Day 50	3	58408	31579